A Numerically Stable Algorithm for the Analysis of Surface Wave Propagation on a Metallic Cylinder Buried in a Biaxially Anisotropic Medium

Julio A. Rams, Guilherme S. Rosa, and Glaucio L. Siqueira

***Abstract*— In this paper, we present a new semi-analytic formulation for analyzing the electromagnetic field propagation along a metallic cylindrical rod immersed in a biaxially anisotropic and lossy media. This geometry can be employed for investigating the propagation around a circular well with important engineering applications for the oil and gas industry. The excitation of surface waves is explored herein by using current loop sources via a spectral domain approach where a novel Hankel-based integral transform is introduced. We present a series of validation results which show that our technique is numerically stable and robust for modeling several representative problems.**

***Keywords*— Surface waves, anisotropic medium, semi-analytic formulation.**

I. Introduction

Surface waves are electromagnetic waves that travel intimately tied to the interface of two different materials [1, Ch. 5]. The majority of the energy of such waves is concentrated close to the interface, rendering a promising mechanism for communication and telemetry for long distances.

Oil and gas industry has many interests on wireless telemetry due its economical advantages compared to the conventional wired technology [2], [3]. The electromagnetic problem usually consider the propagation in two different conditions: a) guided waves inside the production pipe and b) surface waves around the metallic casing of a oil well. Cased boreholes having a tubing string support the propagation of guided waves (in the annular region of the well) but it is strongly affected by losses in the annular region [4]. In contrast, surface waves have been explored by many authors [5]–[7] as a promising communication channel from the Earth's surface to downhole instrumentation. In this case, the propagation is along the surface of a metallic stem embedded in a dispersive hosting rock.

Even though the media around the conductor tube is very lossy, the metallic tube has a much higher refractive index than the surrounding rock. This make it possible to use the interface between the conductor and rock as a single conductor transmission line (SCTL) which is known to support slow surface waves in the axial direction, in such a way that axial currents along the metal tube propagate to the surface where they can be detected, as in Fig. 1.

The authors are with the Center for Telecommunications Studies, Pontifical Catholic University of Rio de Janeiro, Rio de Janeiro 22451-900, Brazil, e-mail: jacostar@cetuc.puc-rio.br. This research was supported in part by the Brazilian Agency FAPERJ under Grant E-26/202.422/2018.

Several computational electromagnetics (CEM) techniques have been used for modeling wave propagation through highly conductive media. This problem, however, requires a robust treatment of the large conductivity contrasts present in complex geophysical formations. In addition, the presence of anisotropic rocks brings more difficulties when we try to solve the Maxwell's equations using brute-force CEM solutions based on finite-elements or finite-differences. High cost computational resources are required for the discretization process and the low-frequency instabilities becomes critical for such large-scale problems.

Bearing in mind the recurring issues of brute-force CEM, the main purpose of this paper is to provide a robust and accurate semi-analytical solution for the analysis of the electromagnetic propagation of surface wave along a metallic cylinder in a biaxial anisotropic medium. The remainder of this paper is organized as follows. In Section II, we introduce the mathematical formulation of the problem via a spectral domain solution. Section III presents the numerical results to validate our technique and demonstrates it accuracy and low cost in terms of CPU time and RAM memory. Finally, Section IV provides the concluding remarks.

II. Formulation Overview

Throughout this work we adopted a notation similar to that used in [8], where the time dependence $e^{-i\omega t}$ is assumed and suppressed. Also, the problem at hand has a geometry with boundaries conformal with cylindrical coordinate surfaces. As a consequence, the cylindrical coordinate system were employed.

The Maxwell's equations in linear, homogeneous and dissipative biaxial anisotropic media satisfy

$$\nabla \times \mathbf{E} = \bar{\bar{z}} \cdot \mathbf{H} - \mathbf{J}_m, \tag{1}$$

$$\nabla \times \mathbf{H} = -\bar{\bar{y}} \cdot \mathbf{E} + \mathbf{J}_e, \tag{2}$$

$$\nabla \cdot (\bar{\bar{\epsilon}} \cdot \mathbf{E}) = \rho_e, \tag{3}$$

$$\nabla \cdot (\bar{\bar{\mu}} \cdot \mathbf{H}) = \rho_m, \tag{4}$$

where $\mathbf{E}$ is the electric field in V/m, $\mathbf{H}$ is the magnetic field in A/m, $\mathbf{J}_e$ is the impressed electric current density in A/m^2 and $\mathbf{J}_m$ is the impressed magnetic current density in V/m^2, ρ_e is the electric charge density in C/m^3, and ρ_m is the magnetic charge density in Wb/m^3. The impeditivity and admitivity tensors are given by $\bar{\bar{z}} = i\omega\bar{\bar{\mu}}$ and $\bar{\bar{y}} = i\omega\bar{\bar{\epsilon}}$, and are expressed in terms of impedance per meter and admittance per meter dimensions, respectively.

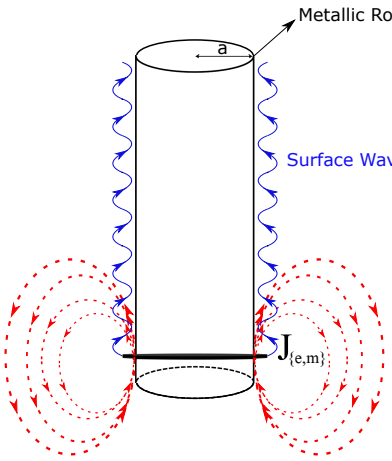

Fig. 1. Current loop antenna radiating in the vicinity of an impenetrable cylinder.

The media is characterized by the complex magnetic permeability and electric permittivity tensors

$$\bar{\bar{\mu}} = \begin{bmatrix} \mu_\rho & 0 & 0 \\ 0 & \mu_\phi & 0 \\ 0 & 0 & \mu_z \end{bmatrix} \quad \text{and} \quad \bar{\bar{\epsilon}} = \begin{bmatrix} \epsilon_\rho & 0 & 0 \\ 0 & \epsilon_\phi & 0 \\ 0 & 0 & \epsilon_z \end{bmatrix}, \tag{5}$$

respectively, with the complex permeability and permittivity

$$\begin{aligned} \mu_{\{\rho,\phi,z\}} &= \mu_0 \mu_{r\{\rho,\phi,z\}}, \text{ and} \\ \epsilon_{\{\rho,\phi,z\}} &= \epsilon_0 \epsilon_{r\{\rho,\phi,z\}} + \frac{i}{\omega}\sigma_{\{\rho,\phi,z\}}. \end{aligned} \tag{6}$$

It can be shown that in case of having the radiation of electric source only or magnetic source only, the vector wave equations satisfied by the electric field or the magnetic field are, respectively

$$\boldsymbol{\nabla} \times \bar{\bar{\mu}}^{-1} \cdot \boldsymbol{\nabla} \times \mathbf{E} - \omega^2 \bar{\bar{\epsilon}} \cdot \mathbf{E} = i\omega \mathbf{J}_e, \quad \text{for} \quad \mathbf{J}_m = \mathbf{0}, \tag{7}$$

$$\boldsymbol{\nabla} \times \bar{\bar{\epsilon}}^{-1} \cdot \boldsymbol{\nabla} \times \mathbf{H} - \omega^2 \bar{\bar{\mu}} \cdot \mathbf{H} = i\omega \mathbf{J}_m, \quad \text{for} \quad \mathbf{J}_e = \mathbf{0}. \tag{8}$$

Mostly induction telemetry systems use transmitter and receiver coils fed by current sources. The main reason for the use coils is that they fit the geometry naturally. Therefore, loop currents antennas are appropriated for the problem in consideration, besides being very simple, cheap and versatile.

Through this work we considered the radiation of electric or magnetic current loops. Because the two problems are dual of each other, the field solutions for a current loop may be easily adapted for the other one.

An electrical or magnetic current loop source (e.g., coil antenna), which is axially symmetric along the z axis, can be expressed as

$$\mathbf{J}_{\{e,m\}} = J_{\{e,m\}} \hat{\phi}. \tag{9}$$

where $J_{\{e,m\}}$ is the azimuthal component of the source.

Let us assume the transmission antenna is an electric or magnetic current loop (filament coil) placed at $\rho = \rho'$ and $z = z'$, and described by the current density

$$J_{\{e,m\}} = I_{\{e,m\}}(\phi)\delta(\rho - \rho')\delta(z - z'), \tag{10}$$

where $I_{\{e,m\}}(\phi)$ is the current distribution in the azimuthal direction and $\delta(\cdot)$ is the Dirac delta.

Under these simplifications, equations (7) and (8) can be recast into a simplified form

$$\left[\frac{p_\rho}{p_z}\frac{\partial}{\partial\rho}\frac{1}{\rho}\frac{\partial}{\partial\rho}\rho + \frac{\partial^2}{\partial z^2} + k^2\right] A_\phi = -i\omega p_\rho I \delta(\rho - \rho')\delta(z - z'), \tag{11}$$

where we have introduced the wavenumber

$$k = \pm\omega\sqrt{q_\phi p_\rho}, \tag{12}$$

and where $A_\phi = E_\phi$, $p = \mu$, $q = \epsilon$, and $I = I_e$ for the electric current loop. In contrast $A_\phi = H_\phi$, $p = \epsilon$, $q = \mu$, and $I = I_m$ for the magnetic current loop. Hence, in a planar, two-dimensional inhomogeneity and excited by an azimuthally independent azimuthal source, the vector wave equations reduce to two simpler scalar wave equations, which determines a transverse electric (TE^z) and transverse magnetic (TM^z) wave to the z direction.

The complete solution for (11) can be constructed by solving first the homogeneous equation, and then by enforcing the jump condition at the source. After some simple but tedious manipulation, we obtain a field solution in terms of the following Hankel-based integral transform:

$$A_\phi = -\frac{\omega p_\rho \rho' I}{2}\int_0^\infty dk_\rho \frac{k_\rho}{k_z}\hat{F}_1(k_\rho\rho)\hat{F}_1(k_\rho\rho')e^{ik_z|z-z'|}, \tag{13}$$

where $\hat{F}_1(k_\rho\rho)$ is defined as

$$\hat{F}_1(k_\rho\rho) = \frac{J_1(k_\rho\rho) + BY_1(k_\rho\rho)}{\sqrt{1 + B^2}}. \tag{14}$$

The axial wavenumber is given by

$$k_z = \pm\sqrt{k^2 - \left(\frac{p_\rho}{p_z}\right)k_\rho^2}, \tag{15}$$

where the square root branch is selecting according to

$$\text{Im}(k_z) > 0, \text{when} \quad z \to +\infty, \text{ and} \tag{16}$$

$$\text{Im}(k_z) < 0, \text{when} \quad z \to -\infty. \tag{17}$$

The above is obtained by enforced the Sommerfeld radiation condition.

The coefficient B in (14) is specified according the radial boundary conditions at $\rho = a$. Without loss of generality, let us assume that the high conductivity cylinder can be well approximated as a perfect electrical conductor (PEC). By imposing the tangential electric field and the normal magnetic flux continuity at the interface $\rho = a$ (over $0 < \phi < 2\pi$ and $-\infty < z < \infty$), we can write [9]

$$\begin{aligned} \hat{\rho} \times \mathbf{E}\big|_{\rho=a} &= \mathbf{0}, \text{ and} \\ \hat{\rho} \cdot \mathbf{B}\big|_{\rho=a} &= 0. \end{aligned} \tag{18}$$

As a result, we can readily find the coefficient B:

$$B = -\frac{J_s(k_\rho a)}{Y_s(k_\rho a)}, \tag{19}$$

where a is the radius of the cylinder, and $s = \{1, 0\}$ for the TE^z and TM^z modal fields, respectively.

It should be observed that the above solution reduces to the one found in [10, eq. 9] for isotropic media. The above formulation can also be employed for modeling sources when the

metallic cylinder is absent. In this scenario, we can verify that B in (14) must be identically null; restoring the conventional Hankel transform usually employed in homogeneous media [8, p. 143].

A. Convergence of the Solution

As can be seen from (13), in order to compute the field quantities, an integral over k_ρ must be calculated. The convergence of the numerical integration plays key influence on the operation speed of the solution.

To accelerate the convergence of the semi-infinite integrals over k_ρ, an adaptive Gauss-Kronrod quadrature algorithm is used. This algorithm attempts to approximate the integral of a scalar-valued function using high-order global adaptive quadrature and default error tolerances, which incorporates less effective points for the integral.

III. Numerical Results

In this section we present some simulation results (via Matlab) obtained using the solution described in (13). The source is modeled as a 10-in-radius electric (magnetic) coil (where 1 in $= 2.54 \times 10^{-2}$ m) with a constant electric (magnetic) current of 1A (1V) that is placed surrounding a metal pipe with radio $a = 9$ in, as in Fig. 1.

These examples are meant to verify and analyze the accuracy of the solution derived. The results were benchmarked against solutions obtained using the COMSOL Multiphysics [11] via a finite element solver.

A. Isotropic Formation

First, we consider an isotropic lossy medium is modeled and described by its electrical conductivity with value 0.5 S/m. The operation frequency for this example is 200 kHz. The relative dielectric and magnetic constants are unity, i.e., the vacuum dielectric and magnetic constants. In Fig. 2 we present the amplitude and phase of the azimuthal component of the electrical (magnetic) field E_ϕ (H_ϕ).

The bigger concentration of samples near the origin in the COMSOL solution is due to the grid selection we made to analyze better the field near the source position.

It is observed that although totally different methods are used, both solutions converge to the same results, validating that the presented solution can accurately model the electromagnetic surface wave propagation excited by a azimuthally symmetric magnetic current loop in a conductive media.

By defining the *attenuation* as

$$\mathrm{Att(dB)} = -20\log_{10}\left|\frac{A(\rho,z)}{A_{\mathrm{source}}}\right|, \qquad (20)$$

where $A(\rho, z)$ represents the magnetic or electric field as a function of the position and A_{source} is such maximum amplitude near the source, we can analyze the dispersion suffered by an electromagnetic wave as a function of the distance away from the source, as in Fig. 3. We also compared the results of the wave propagation in the presence and absence of the metallic cylinder. In Fig. 4 is presented a comparison between these results.

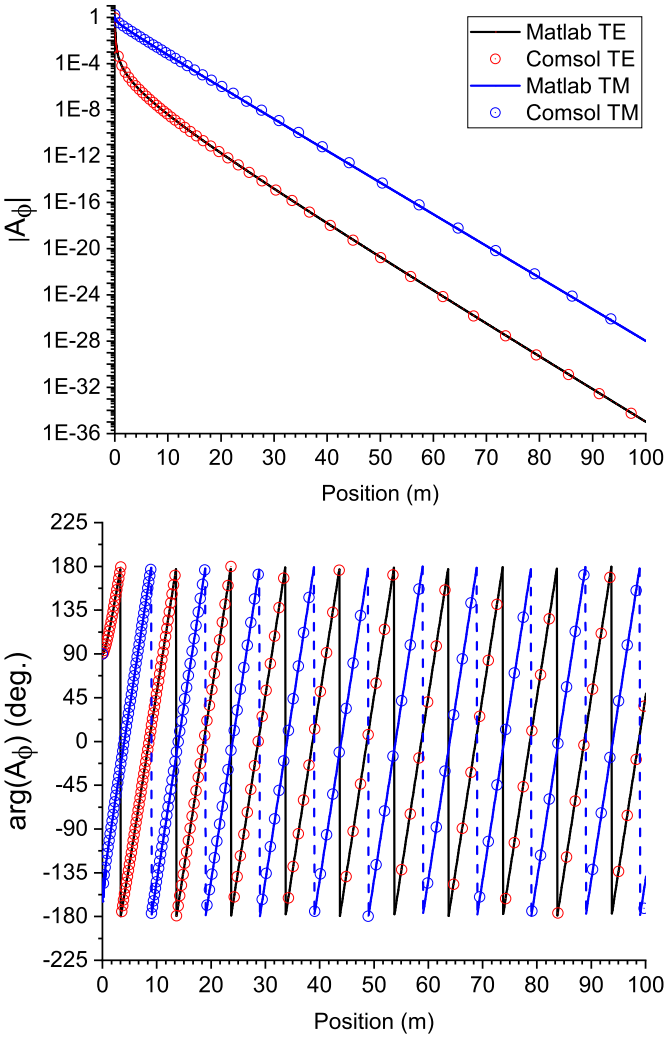

Fig. 2. Absolute and phase values of the azimuthal components of the electrical (magnetic) field E_ϕ (H_ϕ) in an isotropic formation with an embedded cylinder (200 kHz).

It can be noticed that the attenuation for the TM^z reduces drastically due the presence of the metallic cylinder, while for the TE^z mode it increases slightly. If the operation frequency is reduced to 1 kHz, also the attenuation is reduced considerably, as in Fig. 5. The TM^z mode still experiments less attenuation that the TE^z mode when the cylinder is presented.

The presence of the cylinder makes the attenuation of the TM^z mode have a linear behavior, while the TE^z mode has a logarithmic behavior near the source, and far away from it behaves as linear.

In order to visualize the propagation behavior of the electromagnetic field around a finite cylindrical metallic tube of 150 m, Fig. 6 shows the magnitude of the magnetic field component H_ϕ computed with COMSOL at 1 kHz as a function of the radial and the vertical distance from the source (place at $z = 0$). It can be observed that the fields are radially concentrated around the metallic cylinder as a consequence of the high conductivity of the surrounding medium.

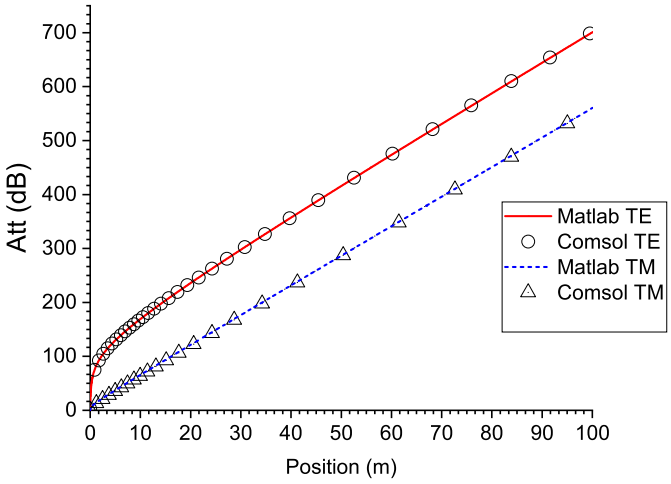

Fig. 3. Attenuation experimented by the azimuthal components of the electrical (magnetic) field E_ϕ (H_ϕ) in an isotropic formation with an embedded cylinder (200 kHz).

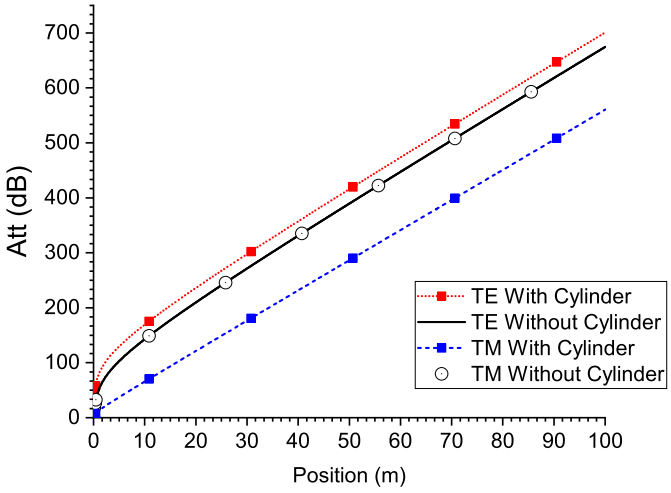

Fig. 4. Comparison of the attenuation experimented by the azimuthal components of the electrical (magnetic) field E_ϕ (H_ϕ) in an isotropic formation with and without the metallic cylinder (200 kHz).

B. Biaxial Anisotropic Formation

In order to analyze the effect of the fully biaxial anisotropy on the wave propagation, we analyze three cases, determined by a permutation of the values in the conductivity tensor, which takes the values of:

$$\bar{\bar{\sigma}}_1 = \begin{bmatrix} 0.5 & 0 & 0 \\ 0 & 0.3 & 0 \\ 0 & 0 & 0.1 \end{bmatrix}, \tag{21}$$

$$\bar{\bar{\sigma}}_2 = \begin{bmatrix} 0.1 & 0 & 0 \\ 0 & 0.5 & 0 \\ 0 & 0 & 0.3 \end{bmatrix}, \tag{22}$$

$$\bar{\bar{\sigma}}_3 = \begin{bmatrix} 0.3 & 0 & 0 \\ 0 & 0.1 & 0 \\ 0 & 0 & 0.5 \end{bmatrix}. \tag{23}$$

The operation frequency for this example is 1 kHz. In Fig. 7 is presented the attenuation experimented by the azimuthal component of the electrical (magnetic) field E_ϕ (H_ϕ) for different anisotropic configurations and the isotropic case.

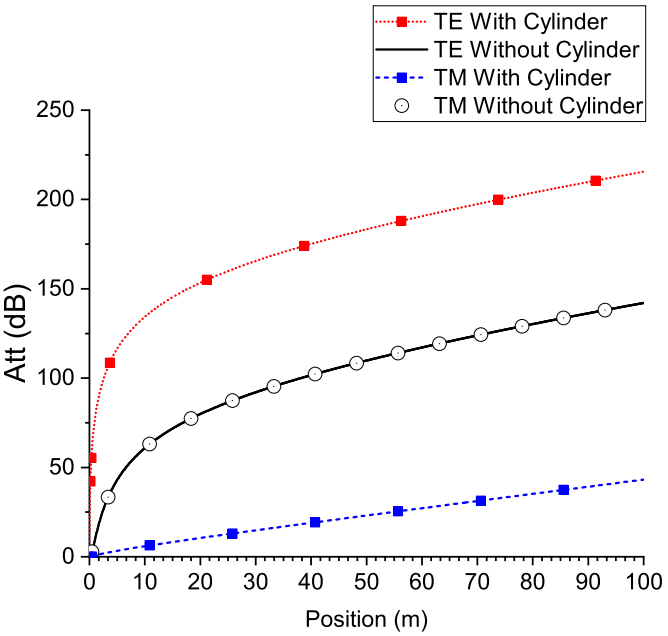

Fig. 5. Comparison of the attenuation experimented by the azimuthal components of the electrical (magnetic) field E_ϕ (H_ϕ) in an isotropic formation with and without the metallic cylinder (1 kHz).

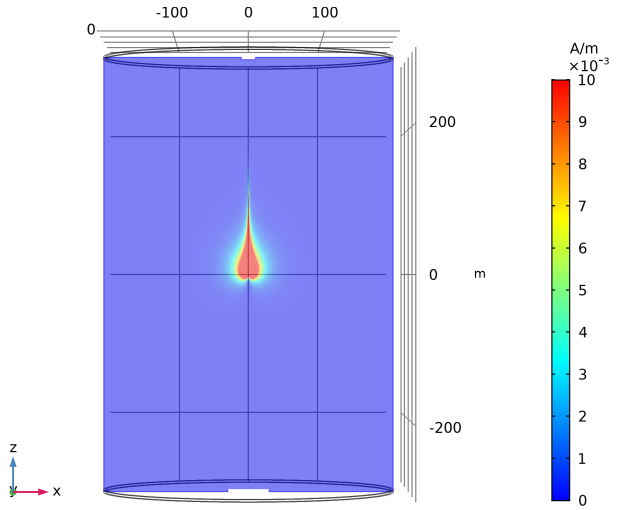

Fig. 6. Azimuthal component of the magnetic field H_ϕ in an isotropic formation with a metallic cylinder (1 kHz) (simulated with COMSOL).

The legend in Fig. 7 is ordered with the smaller attenuation first, for the respective electromagnetic mode. It can be noticed that for the TE^z mode, the attenuation increases as the azimuthal component of the conductivity increases, with independence of the others components. Similarly, for the TM^z mode, the attenuation increases as the radial component of the conductivity increases. This occurs as a consequence of the propagation constant k in (12), that depends just of the azimuthal and radial component of the conductivity tensor for each mode, respectively. When the conductivity component increases, the propagation constant increases, and therefore the attenuation. It is important to note that the attenuation for the TE^z mode with anisotropy described by $\bar{\bar{\sigma}}_2$ is the

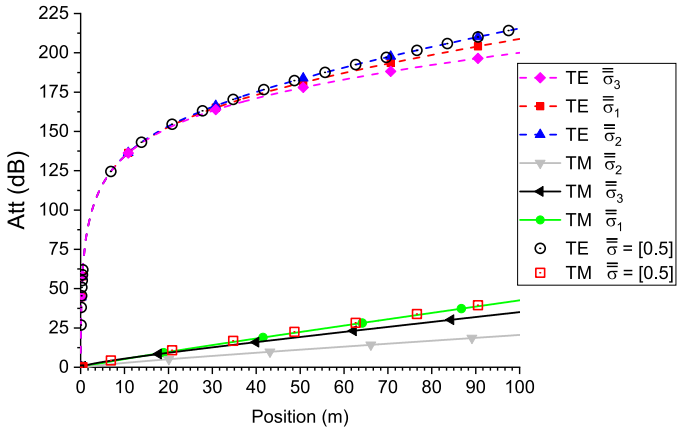

Fig. 7. Attenuation experimented by the azimuthal component of the electrical (magnetic) field E_ϕ (H_ϕ) for different configuration of the anisotropy (1 kHz).

TABLE I
COMPUTATIONAL COSTS OF COMSOL AND THE IMPLEMENTED SOLUTION.

	Our approach	COMSOL
RAM memory	15.78 MB	52.83 GB
CPU time	23.42 s	116.3 s

same as in the isotropic case with conductivity 0.5 S/m. This behavior is due the fact the only component of the electrical permittivity that is involved in the wave equation for the TE^z is the azimuthal one, the others have no effect on the wave propagation.

In Fig. 7 can also be appreciated that the attenuation experimented by the TE^z, regardless of the ordering of the values in the conductivity tensor, is always higher than the attenuation suffered by the TM^z wave. This difference in the attenuation values for both modes is considerable (about 175 dB).

Table I compares the computational costs for COMSOL and the employed solution, from which it can be seen that the provided solution is more computationally efficient. It is important to mention that the solution obtained with COMSOL uses a two-dimensional (2D) axisymmetric modeling, which is less computationally intense when compared with the three-dimensional (3D) model.

IV. CONCLUSIONS

A numerically stable method for solving Maxwell's equation in a biaxially anisotropic media was introduced in this work. To reduce the complexity, the initial 3D problem was simplified to a equivalent 2D one by assuming that the media and the sources are axially symmetric. A novel Hankel-based transform was introduced and we presented a series of validation results against brute-force finite-element solvers that demonstrate the ability of our technique for analyzing surface wave propagation in complex media via a numerically stable and robust semi-analytic algorithm. We have analyzed the effect of the anisotropy in the wave propagation. In addition, we showed that the presence of a metallic tube severely impacts the attenuation of electromagnetic fields. In such scenario, the excitation of TM^z fields is more advantageous compared to TE^z ones.

ACKNOWLEDGMENT

The authors would like to thank Fundação de Amparo à Pesquisa do Estado do Rio de Janeiro (FAPERJ) by the research funding.

REFERENCES

[1] C. A. Balanis, *Advanced engineering electromagnetics*. John Wiley and Sons, Inc., 2 ed., 2012.
[2] M. Y. Xia and Z. Y. Chen, "Attenuation predictions at extremely low frequencies for measurement-while-drilling electromagnetic telemetry system," *IEEE Trans. Geosci. Remote Sens.*, vol. 31, pp. 1222–1228, Nov. 1993.
[3] G. S. Rosa, J. R. Bergmann, and F. L. Teixeira, "Mode-matching modeling of low-frequency wireless telemetry in deep oil fields," in *2017 11th European Conference on Antennas and Propagation (EuCAP)*, (Paris, France), Mar. 19–24 2017.
[4] G. S. Rosa, J. R. Bergmann, and F. L. Teixeira, "Full-wave pseudo-analytical methods for cylindrically symmetric electromagnetic structures: Applications in sensing and telemetry for geophysical exploration," in *Antennas, Antenna Arrays and Microwave Devices: Electromagnetic Analysis and Applications* (T. Bauernfeind, ed.), ch. 10, World Scientific Publishing Co, 2019. To appears. See https://www.worldscientific.com/worldscibooks/10.1142/10987.
[5] S. M. Amjadi and K. Sarabandi, "A compact single conductor transmission line launcher for telemetry in borehole drilling," *IEEE Transactions on Geoscience and Remote Sensing*, vol. PP, pp. 1–8, 01 2017.
[6] M. Gatti, H. Lin, E. Long, J. Sosnowski, and V. Jamnejad, "A test-bed validation of electromagnetic surface wave propagation along a dielectric-coated metal pipe," in *2016 IEEE Aerospace Conference*, pp. 1–13, March 2016.
[7] I. Kotelnikov and G. V. Stupakov, "Electromagnetic surface waves on a conducting cylinder," *Physics Letters A*, vol. 379, 06 2015.
[8] W. C. Chew, *Waves and Fields in Inhomogenous Media*. Wiley-IEEE Press, 1995.
[9] N. I. Sergey V. Yuferev, *Surface Impedance Boundary Conditions. A comprehensive Approach*. CRC Press. Taylor and Francis Group, 2010.
[10] W. C. Chew and B. Anderson, "Propagation of electromagnetic waves through geological beds in a geophysical probing environment," *Radio Science*, vol. 20, pp. 611–621, May 1985.
[11] COMSOL Multiphysics v. 5.4. www.comsol.com. COMSOL AB, Stockholm, Sweden, 2019.